

1 **SOLVING BANG-BANG PROBLEMS USING THE IMMERSED**
2 **INTERFACE METHOD AND INTEGER PROGRAMMING***

3 RYAN H. VOGT* ‡ §, SARAH STRIKWERDA†

4 **Abstract.** In this paper we study numerically solving optimal control problems with bang-bang
5 control functions. We present a formal Lagrangian approach for solving the optimal control problem,
6 and address difficulties encountered when numerically solving the state and adjoint equations by
7 using the immersed interface method. We note that our numerical approach does not approximate
8 the discontinuous control function with smooth functions, instead we solve the true bang-bang op-
9 timal control problem. Our approach for solving the optimal control problem uses an adjoint-based
10 gradient. We use the gradient in our first-order trust-region method to generate a local minimizing
11 control. We present detailed numerical results to demonstrate the effectiveness of our method.

12 **Key words.** ODE-constrained optimization, PDE-constrained optimization, finite-difference
13 methods, immersed-interface method, bang-bang control, optimal control

14 **AMS subject classifications.** 65K10, 49M05, 65M08, 65M12, 90C10

15 **1 Introduction** Optimal control problems are frequently studied due to their
16 importance in a wide range of fields including economics, biological systems, and
17 engineering[1, 2]. In these problems, we seek to find a control that minimizes a cost
18 functional subject to a differential equation. These problems can quickly become very
19 complex. Therefore, in many applications a solution that only takes on a few discrete
20 values is sought after. Such a control is called a bang-bang control. The most common
21 bang-bang control is one which takes on the value of 0 or 1. This is called a bang-
22 bang (on-off) control, and it abruptly changes between extreme values. The change
23 between these values is referred to as a "bang". Bang-bang controls have been used
24 to study how to control the population of invasive species [3], regulate chemotherapy
25 [4], and make decisions about stock options [1].

26 In the current state of the art approaches to solving bang-bang optimal control
27 problems [5, 6, 7], which are a special case of mixed-integer optimal control problems
28 (MIOCPs), several assumptions are made. First, the solution to the different equation
29 constraint is continuous. Second, that when numerically solving the differential equa-
30 tion constraint, the switching points must align with the computational mesh. In this
31 work, we provide a framework to solve bang-bang optimal control problems without
32 assuming regularity in the state, or the computational mesh having to align with the
33 switching points. In this paper we develop finite-difference schemes associated with
34 the bang-bang control problem that are consistent, stable and convergent; using the
35 immersed interface method (IIM). Next we introduce an adjoint-based trust-region
36 method to solve the reduced-space formulation of the bang-bang control problem.

37 We take a formal Lagrangian approach, assuming a reduced-space model. In other
38 words, we assume that given a control v , there exists a unique state T dependent on
39 v . This is to say that the state-to-control operator $T(v)$ is injective. We note that
40 our method can also readily be applied to full-space formulations as well. In our case
41 of a reduced-space formulation, we derive a gradient for v by solving the strong form
42 of the state and adjoint equation. We address the lack of regularity of the state and

*North Carolina State University, Department of Mathematics, rvogt2@ncsu.edu

†North Carolina State University, Department of Mathematics, slstrikw@ncsu.edu

‡Argonne National Laboratory, Mathematics and Computer Science Division

§Lawrence Livermore National Laboratory, Center for Applied Scientific Computing

*Submitted to the editors April 13, 2021.

43 adjoint equation, with IIM. We then use this adjoint-based gradient in a trust-region
 44 method for binary optimization to find a local minimizing bang-bang control.

45 To demonstrate our approach for solving bang-bang problems, we focus on nu-
 46 merically solving the following temperature control problem:

$$\begin{aligned}
 & \underset{T, v}{\text{minimize}} && \frac{1}{2} \int_{\Omega} (T - \hat{T})^2 dt \\
 & \text{subject to} && \frac{dT}{dt} = -K(T - T_s) + Cw + f \quad \text{on } \Omega, \\
 & && \Omega = \bigcup_{i=1}^N \Omega_i, \\
 47 \quad (1.1) & && w(t) = \sum_{i=1}^N v_i \mathbb{1}_{\Omega_i \setminus \partial\Omega_i}(t) \\
 & && , \quad v_i \in \{0, 1\} \quad \forall i = 1 \dots N, \\
 & && \Omega_i = [\tau_i, \tau_{i+1}] \quad \forall i = 1, \dots, N, \\
 & && \tau_1 = 0, \quad \tau_{N+1} = t_{\text{final}}, \\
 & && \Omega = [0, t_{\text{final}}], \\
 & && T(0) = T_0
 \end{aligned}$$

48 where we assume that $T(t)$ is the temperature of a body at time t , $\hat{T}(t)$ is the target
 49 temperature profile, $f \in C(\Omega_i \setminus \partial\Omega_i)$, and $w(t)$ the control function is either "on" or
 50 "off" at a time t . We represent the control function $w(t)$ as a linear combination of
 51 indicator functions $\mathbb{1}$, and assign the control function value to be v_i on $\Omega_i \setminus \partial\Omega_i$. In
 52 this paper we assume that the support of the bang-bang choices, defined by Ω_i , are
 53 equal length i.e.,

$$54 \quad |\Omega_i| = \frac{T}{N}, \quad \forall i = 1 \dots N.$$

55 We also assume that $K, C, t_{\text{final}} > 0$. We note that this assumption does not have
 56 to hold for our method to work; it can very well be the case the the intervals lengths
 57 can vary, but we choose them to be constant length in this work. We lastly note that
 58 we will refer to the objective in this paper as

$$59 \quad (1.2) \quad \mathcal{J} = \frac{1}{2} \int_{\Omega} (T - \hat{T})^2 dt.$$

60 Even though this paper focuses on the specific model problem (1.1), we explain
 61 at each step taken to solve (1.1) how our approach can be tailored to other bang-bang
 62 problems.

63 In this paper we develop a first order, stable convergent method to solve the
 64 state and adjoint equations. The method takes advantage of IIM [8]. The IIM was
 65 originally developed to solve elliptic partial-differential equations with discontinuous
 66 coefficients, also known as interface problems, with a finite-difference approach. The
 67 IIM has been successfully applied to generate high order methods for solving equations
 68 where discontinuities are present [9, 10, 11]. In our work we use the IIM to solve the
 69 adjoint and state equation due to the bang-bang control. We establish a modified

70 Euler's method that can solve the state and adjoint equation, while also obtaining
 71 second order accuracy, stability, and convergence of the numerical solution.

72 In practice, analytic solutions to optimal control problems are difficult to obtain.
 73 In absence of analytic techniques, numerical methods are a powerful tool to solve
 74 optimal control problems. In our example here, the bang-bang control makes it diffi-
 75 cult to apply existing numerical techniques to solve ODE's because $T \notin C^1(\Omega)$. One
 76 at first glance may look at (2.4) and believe that a simple method, such as Euler's
 77 method, may be readily applied to solve the equation numerically. However, Eulers
 78 method assumes that $T \in C^2(\Omega)$ for the method to be applicable. This motivates our
 79 approach of solving the state equation with IIM.

80 We note in our framework the effort of numerically solving the bang-bang problem
 81 lies in solving the differential equations, and building the gradient. The amount of
 82 bangs present in the bang-bang problem, from the perspective of applying our trust-
 83 region method, has little impact on the overall computational effort because we solve
 84 a sequence of binary knapsack problems which can be solved easily.

85 **2 The Lagrangian and the relaxed gradient** To calculate the gradient
 86 of the objective function with the respect to the control parameters v , $\frac{\partial \mathcal{J}}{\partial v}$, we use
 87 a formal Lagrangian approach. We first relax the condition of $v \in \{0, 1\}^N$ to a
 88 continuous relaxation: $0 \leq v \leq 1$. We do this so that we have the notion of a
 89 continuous gradient. However, because this gradient expression is valid for any $0 \leq$
 90 $v \leq 1$, then it will be valid when evaluated at a $v \in \{0, 1\}^N$. We introduce the
 91 Lagrangian:

$$92 \quad (2.1) \quad \mathcal{L}(T, \lambda, v) = \frac{1}{2} \int_{\Omega} (T - \hat{T})^2 dt + \int_{\Omega} \lambda \left(\frac{dT}{dt} + K(T - T_s) - Cw - f \right) dt,$$

94 where λ is the adjoint variable (Lagrangian multiplier).

95 Next we derive the weak state and weak adjoint equations by calculating the
 96 following variational (Gateaux) derivatives:

$$97 \quad \mathcal{L}_{\lambda}[\tilde{\lambda}] = \left. \frac{d}{d\epsilon} \left(\mathcal{L}(T, \lambda + \epsilon \tilde{\lambda}, v) \right) \right|_{\epsilon=0} = 0 \quad (\text{Weak State Equation})$$

$$98 \quad \mathcal{L}_T[\tilde{T}] = \left. \frac{d}{d\epsilon} \left(\mathcal{L}(T + \epsilon \tilde{T}, \lambda, v) \right) \right|_{\epsilon=0} = 0 \quad (\text{Weak Adjoint Equation}).$$

100 The explicit form of these equations are:

$$101 \quad (2.2) \quad \int_{\Omega} \left(\frac{dT}{dt} + K(T - T_s) - Cw - f \right) \tilde{\lambda} dt = 0 \quad \forall \tilde{\lambda} \in H^1(\Omega),$$

$$102 \quad (2.3) \quad \int_{\Omega} \left(-\frac{d\lambda}{dt} + K\lambda + T - \hat{T} \right) \tilde{T} dt = 0 \quad \forall \tilde{T} \in H^1(\Omega)$$

104 The state and adjoint solutions are not $C^1(\Omega)$, however from standard ODE theory
 105 we see the state and adjoint equations are $C^1(\Omega_i \setminus \partial\Omega_i)$. Therefore, we write the
 106 strong form of these equations restricted to the set $\Omega_i \setminus \partial\Omega_i \forall i$:

$$107 \quad (2.4) \quad \begin{cases} \frac{dT}{dt} = -K(T - T_s) + Cw + f & (\text{Restricted Strong State Equation}) \\ T(0) = T_0 \end{cases}$$

108

$$109 \quad (2.5) \quad \begin{cases} -\frac{d\lambda}{dt} = -K\lambda - (T - \hat{T}) + g & (\text{Restricted Strong Adjoint Equation}) \\ \lambda(T) = 0. \end{cases}$$

110 In the remainder of the paper we refer the restricted state and adjoint equations as
 111 just the state and adjoint equations. We note that in the adjoint equation $g = 0$.
 112 However, we include $g \in C(\Omega_i \setminus \partial\Omega_i)$ to test our adjoint solver in Section 9 using the
 113 method of Manufactured Solution and the IIM.

114 The i -th component of the gradient with respect to v_i is then:

$$115 \quad (2.6) \quad \frac{\partial \mathcal{J}}{\partial v_i} = \frac{\partial \mathcal{L}}{\partial v_i} = - \int_{\Omega_i} C \lambda dt.$$

116 So to obtain a gradient associated with a fixed v , we first solve the strong state
 117 equation, then solve the strong adjoint equation. Once we have the adjoint variable,
 118 we then integrate a scaled version it over Ω_i to obtain the i -th component of the
 119 gradient.

120 **3 The discretization of the restricted state Equation** In our optimal
 121 control problem, and other bang-bang problems, the IIM is readily applicable to solve
 122 the state equation. This is because the presence of the bang-bang control can cause,
 123 as seen in (2.4), the state solution to not be $C^1(\Omega)$. However, we can readily apply
 124 the IIM to this problem despite the lack of regularity of the state, or its derivatives,
 125 and have theoretical guarantees that the numerical solution is correct.

126 For many numerical methods, such as Euler or Runge-Kutta, there is an assump-
 127 tion of high regularity in state. Indeed in these methods, the error terms will contain
 128 a high order derivative term. If the solution to an ODE doesn't have the sufficient reg-
 129 ularity to apply these numerical schemes, then one cannot guarantee the consistency
 130 of the method. If the consistency of the numerical method cannot be established then
 131 there is no hope to establish the convergence of the numerical solution to the true so-
 132 lution. This means one cannot be confident that the numerical method approximates
 133 the state solution correctly.

134 In order to apply IIM to the state equation (2.4), we begin by deriving the jump
 135 conditions associated with (2.4). The jump conditions describe how the solution and
 136 it's derivatives jump when a bang occurs. The jump conditions are used to create
 137 our numerical scheme. In our problem, we introduce N binary variables to model the
 138 bang-bang control, so there would be at most $N - 1$ bangs (switches). Each one of
 139 these bangs will occur at

$$140 \quad (3.1) \quad t = \alpha_i = \Omega_i \cap \Omega_{i+1} \quad i = 1, \dots, N - 1.$$

142 For our state scheme, we focus on developing a first-order method, so we need only
 143 to derive the the jump in the state and its first derivative over these bang points.
 144 We note if one wishes to apply the IIM to yield a method of order m , then one must
 145 derive the jump conditions up to the m -th derivative.

146 At each bang time $t = \alpha_i$, we define the jump in the state and its first derivative
 147 to be:

$$148 \quad (3.2) \quad [T]_{t=\alpha_i} = T^+(\alpha_i) - T^-(\alpha_i)$$

$$149 \quad (3.3) \quad \left[\frac{dT}{dt} \right]_{t=\alpha_i} = \frac{dT^+}{dt}(\alpha_i) - \frac{dT^-}{dt}(\alpha_i),$$

151 where we we denote "+" to represent the solution and its derivative to the right of
 152 the bang point and "-" to the left of the bang point. In general we write the k -th
 153 order derivative as:

$$154 \quad \left[\frac{d^k T}{dt^k} \right]_{t=\alpha_i} = \frac{d^k T^+}{dt^k}(\alpha_i) - \frac{d^k T^-}{dt^k}(\alpha_i),$$

155 where we assume that the zero order derivative is just the state itself.

156 In many physical examples, even though the derivative is discontinuous (therefore
157 a non-zero jump) the state is continuous so

$$158 \quad [T]_{t=\alpha_i} = 0.$$

160 This would be known as a direct IIM because we know the jump in the state explicitly.
161 However, in this work we make no such assumption since for general problems there
162 is no manner to know that the state is continuous across the bang points. Therefore
163 in this work we assume it to be unknown i.e

$$164 \quad (3.4) \quad [T]_{t=\alpha_i} = q_i,$$

166 where q_i is to be determined. When the jump conditions are not known explicitly,
167 the method is called the Augmented IIM [11], and q_i for $i = 1, \dots, N - 1$ are called the
168 augmented variables. From (2.4) we see that the jump condition for the derivative of
169 the state is

$$170 \quad (3.5) \quad \left[\frac{dT}{dt} \right]_{t=\alpha_i} = -K[T]_{t=\alpha_i} + C[w]_{t=\alpha_i} + [f]_{t=\alpha_i},$$

172 because we assume K , and T_s to be constant in this work. We then express the jump
173 of the first-derivative in terms of the augmented variables (3.4):

$$174 \quad \left[\frac{dT}{dt} \right]_{t=\alpha_i} = -Kq_i + C[w]_{t=\alpha_i} + [f]_{t=\alpha_i}.$$

176 Next we focus on deriving the IIM scheme for our problem. We discretize the
177 interval $[0, t_{\text{final}}]$ into N_t steps with $t_n = n\Delta t$, $n = 0, \dots, N_t$ and $\Delta t = \frac{t_{\text{final}}}{N_t}$. The idea
178 of the IIM scheme is to use a standard scheme away from the bang points and derive
179 a "corrected" scheme around the bang points to obtain a consistent scheme. In this
180 work we base our scheme around Euler's method. We say that if $t_n \leq \alpha_i \leq t_{n+1}$ for
181 some i then t_n is an irregular grid point. If this is not the case, then the grid point is
182 said to be regular. At regular grid points we apply Euler's method:

$$183 \quad (3.6) \quad T^{n+1} = T^n + \Delta t(-K(T^n - T_s) + Cw^n + f^n) + \mathcal{O}(\Delta t).$$

185 In the case t_n is an irregular grid point we use the method of unknown coefficients:

$$186 \quad (3.7) \quad c_1^n T^{n+1} + c_2^n T^n - \bar{C}^n(c_1, c_2) = -K(T^n - T_s) + Cw^n + f^n + \mathcal{O}(\Delta t),$$

188 where the goal is to find c_1^n , c_2^n and the correction term, $\bar{C}^n(c_1^n, c_2^n)$, that maintains
189 the same order of error as the standard scheme at the irregular grid points, which in
190 this case is first-order accuracy. Since a grid point in our interval is either regular or
191 irregular, we will obtain the order of accuracy of the scheme globally even though the
192 state nor its derivatives need to be continuous on the interval.

193 We use the Taylor series to determine c_1, c_2 and the correction term with first
194 order accuracy. We expand the derivative in terms of the "-" side about α_i :

$$195 \quad (3.8) \quad \frac{dT^-}{dt}(\alpha_i) = c_1 T^{n+1} + c_2 T^n =$$

$$196 \quad c_1^n \left(T^+(\alpha_i) + \frac{dT^+}{dt}(\alpha_i)(t_{n+1} - \alpha_i) + \mathcal{O}\left((t_{n+1} - \alpha_i)^2\right) \right) +$$

$$c_2^n \left(T^-(\alpha_i) + \frac{dT^-}{dt}(\alpha_i)(t_n - \alpha_i) + \mathcal{O}\left((t_n - \alpha_i)^2\right) \right).$$

Note that we expand t_{n+1} in terms of "+" and t_n in terms of "-" because they are to the right and left of the bang point α_i , respectively.

Next we use the jump conditions (3.2) to write T^+ and $\frac{dT^+}{dt}$ in terms of T^- and $\frac{dT^-}{dt}$ so that we can equate the two sides to find c_1, c_2 and the correction term. When equating the two sides, we find that c_1, c_2 satisfy the following system of equation:

$$\begin{aligned} c_1^n + c_2^n &= 0 \\ c_1^n(t_{n+1} - \alpha_i) + c_2^n(t_n - \alpha_i) &= 1, \end{aligned}$$

and the analytic solution to this system is

$$(3.9) \quad c_1^n = \frac{1}{\Delta t}, \quad c_2^n = -\frac{1}{\Delta t}.$$

The corresponding correction term is then

$$(3.10) \quad \bar{C}^n = \frac{1}{\Delta t} \left(q_i + (-Kq_i + c[w]_{t=\alpha_i} + [f]_{t=\alpha_i})(t_n - \alpha_i) \right).$$

4 The discretization of the restricted adjoint equation We build on Section 3 to solve the adjoint equation numerically. Like the state equation, we first derive the jump conditions. Due to the fact that the adjoint equation is solved backwards in time, we introduce the notion of "backward" jump in terms of our previous definitions $[\cdot]_{t=\alpha_i}^{\leftarrow} = -[\cdot]_{t=\alpha_i}$ i.e

$$(4.1) \quad [\lambda]_{t=\alpha_i}^{\leftarrow} = -[\lambda]_{t=\alpha_i} = \lambda^- - \lambda^+ = q_i^\lambda,$$

$$(4.2) \quad \left[\frac{d\lambda}{dt} \right]_{t=\alpha_i}^{\leftarrow} = - \left[\frac{d\lambda}{dt} \right]_{t=\alpha_i} = Kq_i^\lambda - q_i - [g]_{t=\alpha_i}^{\leftarrow},$$

and we introduce a new set of augmented variables q_i^λ that are to be determined. We maintain the same time mesh as the state equation, and move backward instead of forward in time. When moving backwards, from t_n to t_{n-1} , we say t_n is an irregular grid point for the adjoint discretization if $t_{n-1} \leq \alpha_i \leq t_n$, and we say t_n is a regular grid point otherwise. In the case t_n is a regular grid point, we use a backward finite-difference approximation of the adjoint variable's first derivative:

$$\frac{\lambda^n - \lambda^{n-1}}{\Delta t} = -K\lambda^n - (T^n - \hat{T}^n) + g^n + O(\Delta t).$$

For an irregular grid point, we expand on the '+' side, because we are marching backwards:

$$\frac{d\lambda^+}{dt}(\alpha_i) = c_1^{n,\lambda}(\lambda^+(\alpha_i) + \frac{d\lambda^+}{dt}(\alpha_i)(t_n - \alpha_i)) + c_2^{n,\lambda}(\lambda^-(\alpha_i) + \frac{d\lambda^-}{dt}(\alpha_i)(t_{n-1} - \alpha_i)).$$

Like the state equation, we use the method of manufactured coefficients, and the jump conditions for the adjoint variables (4.1) to find the system of equations that $c_1^{n,\lambda}, c_2^{n,\lambda}$ satisfy which we find to be

$$c_1^{n,\lambda} + c_2^{n,\lambda} = 0$$

$$c_1^{n,\lambda}(t_n - \alpha_i) + c_2^{n,\lambda}(t_{n-1} - \alpha_i) = 1.$$

Solving the systems of equations, we find that

$$c_1^{n,\lambda} = -\frac{1}{\Delta t}, \quad c_2^{n,\lambda} = \frac{1}{\Delta t},$$

with corresponding correction term

$$\bar{C}^{n,\lambda} = \frac{1}{\Delta t} \left(q_i^\lambda + (Kq_i^\lambda - q_i - [g]_{t=\alpha_i}^\leftarrow)(t_{n-1} - \alpha_i) \right).$$

The scheme at irregular grid points is then

$$\frac{\lambda^n - \lambda^{n-1}}{\Delta t} + \bar{C}^{n,\lambda} = -K\lambda^n - (T^n - \hat{T}^n) + g^n + O(\Delta t)$$

5 Stability, consistency, and convergence of the state and adjoint finite-difference schemes We must discuss stability, consistence, and convergence of numerical schemes, for regular and irregular grid points independently. Because a grid point is either regular or irregular, by showing stability, consistency, and convergence in each case we show the overall scheme is stable, consistent, and convergent.

In practice, the scheme used for the IIM at regular grid points is a standard method, so the stability, consistency, and convergence of the method is already established. What is left to do is to establish the stability, consistency, and convergence for the scheme at irregular grid points.

In practice, we note that consistency of a method is more readily obtainable than stability. We begin by showing that the numerical scheme is consistent for the state scheme.

PROPOSITION 5.1. *The state scheme is consistent with local truncation error of $\mathcal{O}(\Delta t)$ at both regular and irregular grid points, therefore the method has global truncation error $\mathcal{O}(\Delta t)$.*

Proof. We begin by showing the scheme is consistent at irregular grid points. We substitute the finite difference weights found in (3.9) and correction term, (3.10), into the numerical scheme for the state equation in (3.7). We note that the local truncation error of the method τ becomes

$$\tau = \frac{1}{\Delta t} \mathcal{O}((t_{n+1} - \alpha_i)^2) - \frac{1}{\Delta t} \mathcal{O}((t_n - \alpha_i)^2).$$

We note that at the irregular grid point t_n , $t_n \leq \alpha_i \leq t_{n+1}$, and $t_{n+1} - t_n = \Delta t$. Therefore,

$$\begin{aligned} \tau &= \frac{1}{\Delta t} \mathcal{O}((t_{n+1} - \alpha_i)^2) - \frac{1}{\Delta t} \mathcal{O}((t_n - \alpha_i)^2) \leq \frac{1}{\Delta t} \mathcal{O}(\Delta t^2) - \frac{1}{\Delta t} \mathcal{O}(\Delta t^2) = \mathcal{O}(\Delta t) \\ &\implies \tau = \mathcal{O}(\Delta t), \end{aligned}$$

which is to say that the method is a first-order method at the irregular grid points. We then observe that

$$\lim_{\Delta t \rightarrow 0} \tau = 0,$$

so the method at irregular grid points is consistent as well.

279 Next we refer to [12] to show that the scheme is consistent at regular grid points.
 280 We note that the scheme at regular grid points is the standard forward Euler method.
 281 This scheme has a local truncation error of $\mathcal{O}(\Delta t)$, so the scheme is first-order at
 282 regular grid points, and moreover is consistent because

$$283 \lim_{\Delta t \rightarrow 0} \mathcal{O}(\Delta t) = 0.$$

285 We have shown that the scheme for the state equation is first-order accurate and con-
 286 sistent at both the regular and irregular grid points, so the state scheme is consistent
 287 and first-order accurate. \square

288 We omit a proof that shows the of the adjoint scheme is first-order and consistent
 289 because the argument to prove the result is identical to the state equation proof, just
 290 applied to the adjoint scheme.

291 Next, we show the stability of the state and adjoint schemes by referring to the
 292 literature. In both cases we write the equations in the form:

$$293 \frac{dT}{dt} = \Psi_1(T, t),$$

$$294 \frac{d\lambda}{dt} = \Psi_2(\lambda, T, t).$$

295

297 Because Ψ_1 and Ψ_2 are Lipschitz with respect to the variables T , and λ on $\Omega_i \setminus \partial\Omega_i$
 298 for all $i = 1..N$, then a one step method is stable as shown in [12, Theorem 5.7.1,
 299 p. 345]. Our methods for the state and adjoint scheme are one step methods, and
 300 the correction terms at irregular grid points for both the state and adjoint scheme are
 301 bounded constants (which means Ψ_1 and Ψ_2 are Lipschitz for regular and irregular
 302 grid points) so then the overall scheme is stable.

303 Now we show the convergence of the state and adjoint schemes. We again refer to
 304 the literature, where if a one step method is consistent and stable, then it is convergent
 305 [12, Theorem 5.7.2, p. 348]. Since we have proven the consistency and stability of the
 306 method for both regular and irregular grid points we can establish the convergence
 307 of the solution at regular and irregular grid points due to this theorem. Therefore,
 308 we have established the consistency, stability, and convergence of both the state and
 309 adjoint numerical schemes.

310 We note that in our framework even though the solutions are not continuous
 311 on the entire mesh, it is on the pieces, which allows us to establish the consistency,
 312 stability and convergence of our method due to our IIM approach. If a schemes
 313 consistency, stability, and convergence has been established for differential equations
 314 with high regularity, those proofs can traditionally be altered slightly to establish
 315 these properties for the irregular grid points. To our knowledge this has not been
 316 possible for finite-difference methods applied to bang-bang control problems before
 317 this work.

318 **6 The Discrete State and Adjoint Systems** Suppose we are given a control
 319 v , then augmented IIM for the state equation can be written as the block matrix
 320 system:

$$321 (6.1) \quad \begin{bmatrix} \mathbf{A}_s & \mathbf{B}_s \\ \mathbf{C}_s & \mathbf{D}_s \end{bmatrix} \begin{bmatrix} \mathbf{T} \\ \mathbf{q} \end{bmatrix} = \begin{bmatrix} \mathbf{S}_T \\ \mathbf{S}_q \end{bmatrix},$$

322 where

$$323 \mathbf{A}_s \in \mathbb{R}^{N_t+1 \times N_t+1}, \quad \mathbf{B}_s \in \mathbb{R}^{N_t+1 \times N-1},$$

$$\begin{aligned}
 324 \quad & \mathbf{C}_s \in \mathbb{R}^{N-1 \times N_t+1}, & \mathbf{D}_s & \in \mathbb{R}^{N-1 \times N-1}, \\
 325 \quad & \mathbf{S}_T \in \mathbb{R}^{N_t+1 \times 1}, & \mathbf{S}_q & \in \mathbb{R}^{N-1 \times 1}, \\
 326 \quad & \mathbf{T} \in \mathbb{R}^{N_t+1 \times 1}, & \mathbf{T}_i & = T(t_{i-1}), \quad i = 1, \dots, N_t + 1, \\
 327 \quad & \mathbf{q} \in \mathbb{R}^{N-1 \times 1}, & \mathbf{q}_i & = q_i, \quad i = 1, \dots, N-1.
 \end{aligned}$$

329 In the rows of the upper block of the matrix system we enforce the time step scheme
 330 based on if a row corresponds to an irregular or regular grid point as discussed pre-
 331 viously. In the lower block rows, we enforce the relationship between the state and
 332 state augmented variable for the zero order jump condition.

333 In a similar manner given \mathbf{T}, \mathbf{q} , and control v , augmented IIM for the adjoint
 334 equation can be written as the block matrix system:

$$335 \quad (6.2) \quad \begin{bmatrix} \mathbf{A}_\lambda & \mathbf{B}_\lambda \\ \mathbf{C}_\lambda & \mathbf{D}_\lambda \end{bmatrix} \begin{bmatrix} \boldsymbol{\lambda} \\ \mathbf{q}^\lambda \end{bmatrix} = \begin{bmatrix} \mathbf{S}_\lambda \\ \mathbf{S}_{q^\lambda} \end{bmatrix},$$

336 where

$$\begin{aligned}
 337 \quad & \mathbf{A}_\lambda \in \mathbb{R}^{N_t+1 \times N_t+1}, & \mathbf{B}_\lambda & \in \mathbb{R}^{N_t+1 \times N-1}, \\
 338 \quad & \mathbf{C}_\lambda \in \mathbb{R}^{N-1, N_t+1}, & \mathbf{D}_\lambda & \in \mathbb{R}^{N-1 \times N-1}, \\
 339 \quad & \mathbf{S}_\lambda \in \mathbb{R}^{N_t+1 \times 1}, & \mathbf{S}_{q^\lambda} & \in \mathbb{R}^{N-1 \times 1}, \\
 340 \quad & \boldsymbol{\lambda} \in \mathbb{R}^{N_t+1 \times 1} & \boldsymbol{\lambda}_i & = \lambda(t_{N_t-i+1}), \quad i = 1, \dots, N_t + 1, \\
 341 \quad & \mathbf{q}^\lambda \in \mathbb{R}^{N-1 \times 1} & \mathbf{q}^\lambda_i & = q_i^\lambda, \quad i = 1, \dots, N-1.
 \end{aligned}$$

343 Like in the case of the state equation, we enforce the scheme at regular and irregular
 344 grid points in the upper block, and in the lower block enforce the augmented variable
 345 on the state.

346 A consideration of this paper is not to derive appropriate preconditions to apply
 347 to the augmented state or augmented adjoint systems. However, constructing such
 348 a preconditioner would help speed up the computational time required to solve the
 349 systems.

350 **7 Discretization of The Objective Function and Gradient** In Section 6,
 351 we wrote the discretization schemes to produce a discretized state solution \mathbf{T} , and
 352 discretized adjoint solution $\boldsymbol{\lambda}$, for a fixed control v . In this section we show how we
 353 produce an objective function value and gradient for these discretized solutions.

354 In our optimal control problem the objective function is:

$$355 \quad \frac{1}{2} \int_{\Omega} (T - \hat{T})^2 dt.$$

356 We approximate the objective function with the trapezoid rule:

$$357 \quad (7.1) \quad \mathcal{J} = \frac{1}{2} \int_{\Omega} (T - \hat{T})^2 dt = \int_{\Omega} \hat{f}(t) dt = \sum_{i=1}^{N_t} \frac{\Delta t}{2} \left(\hat{f}(t_{i-1}) + \hat{f}(t_i) \right) + \mathcal{O}(\Delta t^2),$$

358 where

$$359 \quad (7.2) \quad \hat{f}(t) = \frac{1}{2} (T(t) - \hat{T}(t))^2.$$

360 For simplicity of notation, we define the numerical approximation of the objective
361 function to be

$$362 \quad (7.3) \quad \hat{J}^{\Delta t} = \sum_{i=1}^{N_t} \frac{\Delta t}{2} \left(\hat{f}(t_{i-1}) + \hat{f}(t_i) \right).$$

363 We approximate the i -th component of the gradient, associated with the binary
364 variable v_i , using the trapezoid rule:

$$365 \quad (7.4) \quad \frac{\partial \mathcal{J}}{\partial v_i} = - \int_{\Omega_i} C \lambda dt = \int_{\Omega_i} \hat{g}(t) dt = \sum_{k=1}^{\hat{N}_t^i} \frac{\Delta t}{2} \left(\hat{g}(\hat{t}_{k-1}) + \hat{g}(\hat{t}_k) \right) + \mathcal{O}(\Delta t^2),$$

366 where

$$367 \quad (7.5) \quad \hat{g}(t) = -C \lambda(t).$$

368 The notation \hat{N}_t^i corresponds to the number of time steps in the mesh that exist
369 within Ω_i , and \hat{t} corresponds to the specific time steps that exist in Ω_i . Again, for
370 simplicity of notation, we define the numerical approximation of i -th component of
371 the gradient vector to be

$$372 \quad (7.6) \quad \left(g_{\Delta t} \right)_i = \sum_{k=1}^{\hat{N}_t^i} \frac{\Delta t}{2} \left(\hat{g}(\hat{t}_{k-1}) + \hat{g}(\hat{t}_k) \right)$$

373 **8 A trust-region method for bang-bang control** In [13], a trust-region
374 method is introduced to solve binary partial-differential equation constrained opti-
375 mization problems. We note that this method is readily applicable to our problem,
376 and is outlined in Algorithm 8.1. The algorithm can be viewed as solving a sequence
377 of differential equations and binary knapsack problems to yield a local minimizing
378 binary control. A strength of this algorithm is that the computational effort is not
379 bottlenecked by the number of binary variables present in the optimal control prob-
380 lem. This is because the binary variables appear in the trust-region subproblem; the
381 trust-region subproblem is a knapsack problem, so it is computationally inexpensive
382 to solve even for a large amount of binary variables. Instead, the computational effort
383 required to execute the trust-region method is focused on solving the state and adjoint
384 equation, and then building the gradient.

385 **9 Numerical experiments** We provide numerical evidence that our approach
386 to solve the bang-bang state equation, using IIM, provides the correct numerical
387 solution. In our simulations, we solve 2.4 with parameters $f = 0$, $C = 3$, $K =$
388 1 , $T_0 = 70$, $T_s = 50$, $t_{\text{final}} = 10$, $N = 10$., and choose v in the following manner:

$$389 \quad (9.1) \quad \begin{cases} v_i = 1 & i \text{ is odd} \\ v_i = 0 & i \text{ is even,} \end{cases}$$

390 for $i = 1, \dots, N$. In this instance, we can derive the exact solution to the state equation:

$$391 \quad (9.2) \quad T_{\text{true}}(t) = \begin{cases} T_0 e^{-Kt} + T_s - T_s e^{-Kt} + \frac{C}{K} - \frac{C}{K} e^{-Kt} & t \in \Omega_i, i \text{ is odd} \\ T_0 e^{-Kt} + T_s - T_s e^{-Kt} & t \in \Omega_i, i \text{ is even.} \end{cases}$$

Algorithm 8.1 Steepest-Descent Trust-Region Algorithm.

Given initial trust-region radius $\Delta_0 = \bar{\Delta} \geq 1$ and initial guess $v^{(0)} \in \{0, 1\}^N$

Select an acceptance step parameter $\bar{\rho}$, and set $k \leftarrow 0$

Evaluate the objective function $\hat{J}_{\Delta t}^{(k)} = \hat{J}^{\Delta t}(v^{(k)})$ and the gradient $g_{\Delta t}^{(k)} = \nabla_v \hat{J}^{\Delta t}(v^{(k)})$

while $\Delta_k \geq 1$ **do**

Solve the trust-region (knapsack) subproblem for \hat{v} :

$$\begin{aligned} \hat{v} = \underset{v}{\text{minimize}} \quad & g_{\Delta t}^{(k)T} (v - v^{(k)}) + \hat{J}_{\Delta t}^{(k)} \\ & \|v - v^{(k)}\|_1 \leq \Delta_k \\ & v \in \{0, 1\}^N \end{aligned}$$

Evaluate the objective $\hat{J}_{\Delta t}(\hat{v}, T(\hat{v}))$ by solving state equations with \hat{v}

Compute the ratio of actual over predicted reduction: $\rho_k = \frac{\hat{J}_{\Delta t}^{(k)} - \hat{J}_{\Delta t}(\hat{v}, \psi(\hat{v}))}{-(g_{\Delta t}^{(k)})^T (\hat{v} - v^{(k)})}$

if $\rho_k > \bar{\rho}$ **then**

Accept the step: $v^{(k+1)} = \hat{v}$, and evaluate the gradient $g_{\Delta t}^{(k+1)} = \hat{J}'(v^{(k+1)})$

if $\|v^{(k+1)} - v^{(k)}\|_1 = \Delta_k$, **then** increase the trust-region radius $\Delta_{k+1} = 2\Delta_k$;

else if $\rho_k > 0$ **then**

Accept the step $v^{(k+1)} = \hat{v}$, and evaluate the gradient $g_{\Delta t}^{(k+1)} = \hat{J}'(v^{(k+1)})$

Keep trust-region radius unchanged $\Delta_{k+1} = \Delta_k$

else

Reject the step, set $v^{(k+1)} = v^{(k)}$, and copy the gradient $g_{\Delta t}^{(k+1)} = g_{\Delta t}^{(k)}$

Reduce the trust-region radius $\Delta_{k+1} = \text{floor} \left(\frac{\Delta_k}{2} \right)$

Set $k \leftarrow k + 1$

392 We numerically solve 2.4 in several instances containing a different number of time
 393 steps i.e $N_t = 2^p$ for $p = 5..11$ using both Eulers method and our IIM approach. We
 394 record the maximal of the absolute error between the numerical and true solution in
 395 each simulation, and calculate the convergence order as we refine the mesh for both
 396 Euler method and our IIM approach; we show these results in Table 1. We note that
 397 we calculate the error in the infinity norm, and the convergence γ^* by:

$$\gamma^* = \frac{\log \left(\frac{E_{N_t}^*}{E_{N_t}^* / 2} \right)}{\log(2)}.$$

400 In the IIM approach [11], we expect the average convergence order to reflect the
 401 overall convergence of the method. If we average the convergence order for the IIM
 402 approach in 1, we see that the order of the method does indeed reflect a convergence
 403 order of 1. In comparison, as we observe the convergence order for Euler's method,
 404 we see that the convergence order average is not close to 1. Instead, as we refine
 405 the mesh the convergence order is approaching 0. This is not surprising, because the
 406 theoretical assumption to use Euler's method is $T \in C^2(\Omega)$, which is violated in this
 407 case. In the absence of such an assumption, one cannot guarantee the consistency,
 408 let alone the convergence of the numerical method. In Figure 1, we visually show
 409 the solutions generated from the IIM and Euler approach. We observe that the IIM
 410 captures the jumps in the state solution due to the bang-bang control, while Euler's

411 method does capture these jumps accurately. It is crucial to solve the state equation
 412 correctly, and as we have demonstrated, the introduction of bang-bang controls will
 413 cause traditional numerical methods for ordinary-differential equations to fail.

414 On the optimal control front, being unable to solve the state equation correctly
 415 undoubtedly produces an incorrect adjoint solution. It should come as no surprise
 416 that the gradient, which is calculated with this incorrect state and adjoint solution,
 417 also will be incorrect. In Table 2 we demonstrate what occurs when we use the IIM
 418 approach to calculate the state and adjoint equation. We first observe that both the
 419 state and the adjoint solutions achieve first-order convergence. This is to say that the
 420 state solution is first order accurate, but also when we pass this solution to the adjoint
 421 equation and use the IIM approach we maintain the first order accuracy. We use the
 422 state and adjoint solution to then create a gradient. In the table, we compare the
 423 difference of the gradient and the a forward difference approximation of the gradient
 424 in the infinity norm. We observe that the gradient also obtains first order convergence,
 425 which is expected. Our results demonstrate that not only using our IIM approach
 426 solves the state and adjoint equation in the presence of bang-bang control correctly,
 427 but also that the gradient produced by using the IIM generated state and adjoint
 428 solution is consistent.

429 Since we have shown that our approach creates a consistent gradient, we now
 430 share results for our trust-region method applied to the problem. In our runs, we let
 431 $T_0 = 10$, $T_s = 0$, $K = 0.1$, $C = 2$, $f = 0$, $g = 0$ and $t_{\text{final}} = 100$. In our numerical tests,
 432 we let $\hat{T}(t) = 5 + 0.5 \sin(t)$. We test the trust-region method when the number of
 433 bangs are 100, 1000, and 10000. For all simulations we pick $N_t = 20000$ to guarantee
 434 a resolved bang-bang control for all the scenarios mentioned.

435 To execute our trust-region method, we need a feasible starting guess. While a
 436 random binary solution would be sufficient, in [13] it was observed that solving the
 437 relaxation of the problem ($0 \leq v \leq 1$) and then rounding was produced a minimum
 438 with lower objective function value. We choose to use the simple rounding heuristic:

$$439 \quad [v_{\text{round}}]_i = \begin{cases} 0 & v_i < 1 \\ 1 & v_i \geq 1. \end{cases}$$

440

441 In Table 3 we report the computational effort required to solve the relaxation,
 442 the number of trust-region iterations required to find a minimizing solution, and the
 443 total time required to do the two pieces of the trust region method: solving the
 444 state and adjoint equation then constructing the gradient and executing the trust-
 445 region subproblem. We observe the amount of time taken to solve the knapsack
 446 problem is computationally negligible when compared to the time required to build a
 447 gradient. This means that with our trust-region method for binary optimization the
 448 bottleneck is the bottleneck of doing classical optimal control; we observe that the
 449 binary variables are almost inconsequential. Solving the adjoint and state equation
 450 in the most efficient manner possible is out of the scope of this work, but we note
 451 that carefully constructed preconditioners for the state and adjoint equation can also
 452 drastically decrease the computational time to solve the state and adjoint systems.

453 In Figure 2, we show the progress of the trust-region methods radius and objective-
 454 function value as a function of iteration count. We observe that as we increase the
 455 amount of bangs present, we increase the amount of trust-region iterations required
 456 to find a minimizing solution. Moreover we reduce the objective-function value quite
 457 quickly early in execution of the trust-region method, but then see slow convergence
 458 to a local minimum; an artifact of the non-convexity of the objective function.

459 In Table 4 we report the objective function value and in Figure 3 we show the
 460 optimal control, state, and target function for a different amount of bang controls. In
 461 the table, we see that we are able to make a significant percent reduction in all cases,
 462 and that the percent reduction is observed to be greater when more bangs are present.
 463 In the figure, we observe that we are successful at producing controls that create states
 464 which model the behavior of the target we are attempting to match. We observe that
 465 as we increase the number of bangs, we find an optimal control that makes the state
 466 model the target function more accurately. These results indicate that using our IIM
 467 approach, combined with an adjoint based gradient and trust-region method, does
 468 indeed yield a successful control strategy.

Table 1: Error (E) and convergence (γ) table for Euler (superscript E) method and the IIM (superscript IIM) approach applied to the state equation 2.4.

N_t	IIM		Euler Method	
	$E_{N_t}^{\text{IIM}}$	$\gamma_{N_t}^{\text{IIM}}$	$E_{N_t}^{\text{E}}$	$\gamma_{N_t}^{\text{E}}$
32	3.140		3.140	
64	1.255	1.322	1.517	1.048
128	0.574	1.124	1.431	0.084
256	1.497	-1.382	1.369	0.064
512	0.135	3.467	1.329	0.042
1024	0.067	1.013	1.328	0.001
2048	0.034	0.944	1.323	0.005

Table 2: Error and convergence table for the state, adjoint and gradient .

N_t	State		Adjoint		Gradient	
	$E_{N_t}^{\text{IIM}}$	$\gamma_{N_t}^{\text{IIM}}$	$E_{N_t}^{\text{IIM}}$	$\gamma_{N_t}^{\text{IIM}}$	$E_{N_t}^{\text{IIM}}$	$\gamma_{N_t}^{\text{IIM}}$
32	19.834		44.528		36.177	
64	7.607	1.382	9.945	2.162	19.417	0.897
128	3.375	1.172	4.283	1.215	9.933	0.966
256	1.678	1.008	1.369	1.126	4.919	1.013
512	0.832	1.011	1.329	1.090	2.517	0.966
1024	0.415	1.005	0.448	1.039	1.263	0.994
2048	0.207	1.006	0.223	1.007	0.632	0.998

469 **10 Solving general binary bang-bang problems with our approach** In
 470 this Section we summarize how the our approach can be applied to more general
 471 reduced space binary bang-bang problems. We discuss the three key components in
 472 as much generality as possible : building the Lagrangian, building the IIM schemes
 473 for the state and adjoint system, and applying the trust-region method.
 474 **Construct a Lagrangian.**
 475 Suppose we have a bang-bang optimal control problem of the form:

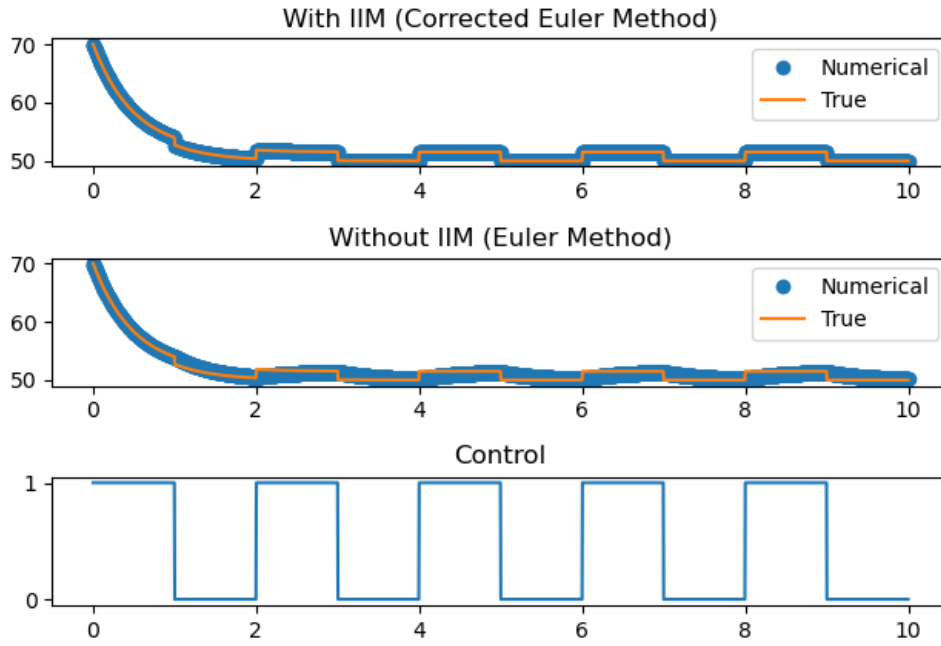


Fig. 1: Comparison of the numerical solution yielded by the IIM and Euler method to the exact solution for a fixed bang-bang control for $N_t = 2048$ from Table

Table 3: For 100, 1000, and 10000 binary variables we record the CPU times(s) for solving the relaxation to initialize the trust-region method. In addition we record the CPU times(s) for computing the state, adjoint, and gradient; in addition to the time required to executing the trust-region sub problems (knapsack problems). These times are reflective of the amount of trust-region iterations required to find a minimizing bang-bang control.

Number of Bangs	Solution CPU Time(s)			Trust-Region Iterations
	Relaxation	ODEs/Gradient	MIPs	
100	7999.89	9372.31	1.31	18
1000	5270.65	72173.45	8.70	128
10000	5637.85	720508.67	218.09	415

$$\begin{aligned}
 & \underset{T, v}{\text{minimize}} && \mathcal{J}(T(v), v) \\
 & \text{subject to} && C(T, v) = 0 \quad \text{on } \Omega, \\
 & && \Omega = \bigcup_{i=1}^N \Omega_i, \\
 & && w(t) = \sum_{i=1}^N v_i \mathbb{1}_{\Omega_i \setminus \partial \Omega_i}(t) \\
 & && v_i \in \{0, 1\} \quad \forall i = 1 \dots N, \\
 & && \Omega_i = [\tau_i, \tau_{i+1}] \quad \forall i = 1, \dots, N, \\
 & && \tau_1 = 0, \quad \tau_{N+1} = t_{\text{final}}, \\
 & && \Omega = [0, t_{\text{final}}], \\
 & && T(0) = T_0.
 \end{aligned}
 \tag{10.1}$$

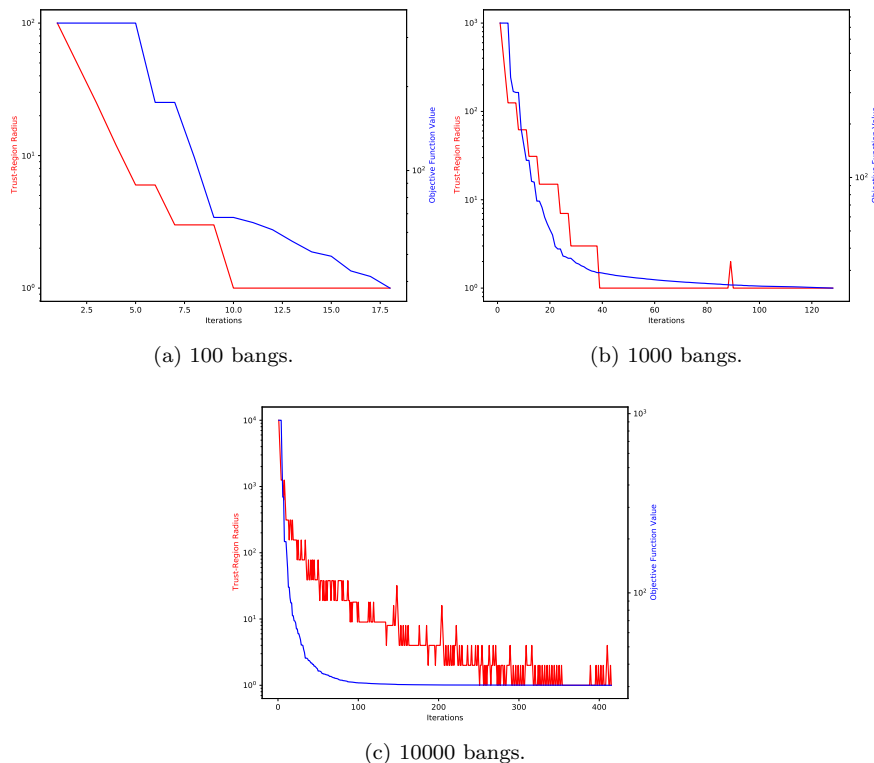


Fig. 2: Trust-region method objective function value and trust-region radius evolution for 100,1000, and 10000 binary variables. On the left axis (red) we plot the objective function value as a function of iteration count, and on the right axis (blue) we plot the trust-region radius as a function of iteration count.

Table 4: The objective function value before (OFVB) at the rounded relaxation (start of trust-region), objective function value after (OFVA) at the termination of trust-region, and the percent-reduction in the objective function value from the start to end of the trust-region method for 100, 1000 and 10000 binary variables.

Number of Bangs	OFVB	OFVA	Percent Reduction (%)
100	337.93	37.93	88.77
1000	739.24	23.84	96.77
10000	918.76	30.50	96.68

477 Where $C : t \rightarrow \mathbb{R}^k$, $k \geq 1$. We define an adjoint variable, $\lambda : t \rightarrow \mathbb{R}^k$, and define the
 478 Lagrangian

479 (10.2)
$$\mathcal{L}(T, \lambda, v) = \mathcal{J} + \int_{\Omega} \lambda^T C dt.$$

480 From the Lagrangian, we derive the restricted state and adjoint equation, and the
 481 gradient, as seen in Section 2. We note that if there are additional constraints on the

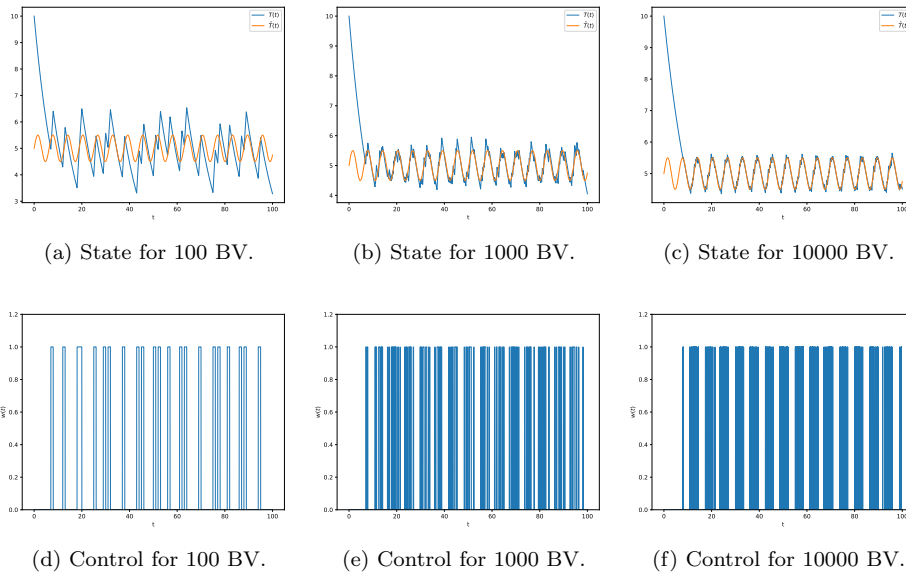


Fig. 3: Plots of the state $T(t)$, target $\hat{T}(t) = 5 + 0.5 \sin(t)$, and bang control $w(t)$ for 100, 1000, and 10000 binary variables (BV).

482 binary variable, which is not considered in our formulation, these constraints can be
 483 ignored in the Lagrangian and instead enforced in the trust-region subproblem.

484 **Derive the augmented IIM Schemes for the state and adjoint system.**

485 Next, the state and adjoint problem are discretized using the IIM approach. Typically,
 486 we use a standard numerical method (in this paper Euler), as a foundation to construct
 487 a "corrected" scheme with the IIM approach. One can view our approach as the
 488 standard scheme being applied at regular grid points, while the "corrected" scheme
 489 is applied at irregular grid points. If the scheme that is used at the regular grid
 490 points has been shown to be consistent, stable, and convergent, then the scheme at
 491 the irregular grid points consistency, stability, and convergence proofs need to be only
 492 slightly altered. Having a methods that are consistent, stable, and convergent for
 493 the state and adjoint equation are critical. Because without the correct state and
 494 adjoint computation, it is impossible to have a consistent gradient, let alone to solve
 495 the overarching optimal control problem with any numerical optimization approach.

496 **Apply the trust-region method.** In our work we first solve the relaxation of
 497 our optimal control problem, and then round the relaxation to produce a feasible
 498 starting guess to the binary optimal control problem. In our previous work, [13] we
 499 have observed that initializing our trust-region method with the rounded relaxation
 500 produced controls that yield lower objective function value than we when initialized
 501 our initial trust-region method with a random binary guess. Our trust-region methods
 502 computational effort is bottle-necked by only the state and adjoint computation, which
 503 one would have to perform for any reduced space optimal control problem. However,
 504 regardless of the amount of binary variables present in the problem we can solve the
 505 trust-region sub problem quickly.

506 **11 Conclusions** In this work, we introduced a formal Lagrangian approach
 507 for solving bang-bang optimal control problems. We introduced a target optimal
 508 control and wrote the optimality conditions, which led to solving the state and adjoint
 509 equation using IMM to ensure that we obtain a numerical solutions that are consistent,
 510 stable, and convergent. By solving the state and adjoint equation we are able to
 511 produce a gradient, and an objective function value that is associated with a fixed
 512 bang-bang control. We use the objective function value and gradient to execute our
 513 trust-region method. We showed numerical simulations that both demonstrated the
 514 importance of not applying standard numerical methods to the state equation, but
 515 also that our approach generates bang-bang controls that meets our goals. This work
 516 provides a blueprint that readers can use to as a foundation to solve their own bang-
 517 bang problems quickly and efficiently.

518 **12 Acknowledgements** This document was prepared as an account of work
 519 sponsored by an agency of the United States government. Neither the United States
 520 government nor Lawrence Livermore National Security, LLC, nor any of their em-
 521 ployees makes any warranty, expressed or implied, or assumes any legal liability or
 522 responsibility for the accuracy, completeness, or usefulness of any information, ap-
 523 paratus, product, or process disclosed, or represents that its use would not infringe
 524 privately owned rights. Reference herein to any specific commercial product, process,
 525 or service by trade name, trademark, manufacturer, or otherwise does not necessar-
 526 ily constitute or imply its endorsement, recommendation, or favoring by the United
 527 States government or Lawrence Livermore National Security, LLC. The views and
 528 opinions of authors expressed herein do not necessarily state or reflect those of the
 529 United States government or Lawrence Livermore National Security, LLC, and shall
 530 not be used for advertising or product endorsement purposes. This document has
 531 been approved to be released for widespread consumption according to order LLNL-
 532 JRNL-821389.

533

REFERENCES

- 534 [1] Ping Chen and Sardar MN Islam. *Optimal control models in finance*. Springer, 2005.
- 535 [2] U. Ledzewicz and H. Schättler. Optimal control for a bilinear model with recruiting agent in
 536 cancer chemotherapy. In *42nd IEEE International Conference on Decision and Control*
 537 *(IEEE Cat. No.03CH37475)*, volume 3, pages 2762–2767 Vol.3, 2003.
- 538 [3] PDN Srinivasu and BSRV Prasad. Role of quantity of additional food to predators as a control
 539 in predator–prey systems with relevance to pest management and biological conservation.
 540 *Bulletin of mathematical biology*, 73(10):2249–2276, 2011.
- 541 [4] Shuo Wang and Heinz Schättler. Optimal control of a mathematical model for cancer chemo-
 542 therapy under tumor heterogeneity. *Mathematical Biosciences & Engineering*, 13(6):1223,
 543 2016.
- 544 [5] Felix Bestehorn, Christoph Hansknecht, Christian Kirches, and Paul Manns. A switching cost
 545 aware rounding method for relaxations of mixed-integer optimal control problems. In *2019*
 546 *IEEE 58th Conference on Decision and Control (CDC)*, pages 7134–7139. IEEE, 2019.
- 547 [6] Marcel Antal, Claudia Pop, Tudor Cioara, Ionut Anghel, Ionut Tamas, and Ioan Salomie.
 548 Proactive day-ahead data center operation scheduling for energy efficiency: Solving a miocp
 549 using a multi-gene genetic algorithm. In *2017 13th IEEE International Conference on*
 550 *Intelligent Computer Communication and Processing (ICCP)*, pages 527–534. IEEE, 2017.
- 551 [7] Alberto De Marchi. On the mixed-integer linear-quadratic optimal control with switching cost.
 552 *IEEE Control Systems Letters*, 3(4):990–995, 2019.
- 553 [8] Randall J Leveque and Zhilin Li. The immersed interface method for elliptic equations with
 554 discontinuous coefficients and singular sources. *SIAM Journal on Numerical Analysis*,
 555 31(4):1019–1044, 1994.
- 556 [9] Mark N Linnick and Hermann F Fasel. A high-order immersed interface method for simulating
 557 unsteady incompressible flows on irregular domains. *Journal of Computational Physics*,

- 558 204(1):157–192, 2005.
- 559 [10] Long Lee and Randall J LeVeque. An immersed interface method for incompressible navier–
560 stokes equations. *SIAM Journal on Scientific Computing*, 25(3):832–856, 2003.
- 561 [11] Zhilin Li and Ming-Chih Lai. The immersed interface method for the navier–stokes equations
562 with singular forces. *Journal of Computational Physics*, 171(2):822–842, 2001.
- 563 [12] Walter Gautschi. *Numerical analysis*. Springer Science & Business Media, 1997.
- 564 [13] Ryan H Vogt, Sven Leyffer, and Todd Munson. A mixed-integer PDE-constrained optimization
565 formulation for electromagnetic cloaking. 2020.

566 **Acknowledgements** This material was based upon work supported by the U.S.
567 Department of Energy, Office of Science, Office of Advanced Scientific Computing Re-
568 search, Scientific Discovery through Advanced Computing (SciDAC) program through
569 the FASTMath Institute under Contract DE-AC02-06CH11357 at Argonne National
570 Laboratory. This work was also supported by the U.S. Department of Energy through
571 grant DE-FG02-05ER25694.